# Highlights

# A modified Rittinger model for the grinding of wet granular material

Mathis Thouret, Claire Mayer-Laigle, Vincent Richefeu, Komlanvi Lampoh, Jean-Yves Delenne

- The grinding of quartz sand was performed in a vibratory ball mill across the full range of water contents, from dry to saturated samples.
- The grinding rate shows a strong correlation with the Carr index, which measures the densification capacity of a granular bed.
- A modified Rittinger model, incorporating water content through the evolution of the Carr index, was proposed.

# A modified Rittinger model for the grinding of wet granular material\*

Mathis Thouret<sup>a,\*</sup>, Claire Mayer-Laigle<sup>a,\*\*</sup>, Vincent Richefeu<sup>b</sup>, Komlanvi Lampoh<sup>a</sup> and Jean-Yves Delenne<sup>a</sup>

<sup>a</sup>IATE, Univ. Montpellier, INRAE, Institut Agro, Montpellier, France <sup>b</sup>3SR, Univ. Grenoble Alpes, Grenoble INP, CNRS, Grenoble, France

#### ARTICLE INFO

#### Keywords: Unsaturated granular media Wet comminution Carr index Grinding energy Modified Rittinger model

#### ABSTRACT

Grinding is a fundamental process widely used across various industrial sectors. Although often considered merely a pre-treatment step, it remains poorly studied from a fundamental perspective-especially when accounting for the presence of water or humidity. In particular, the relationship between grinding parameters and size reduction efficiency remains a critical bottleneck in optimizing this highly energy-intensive operation. The water content of the raw material to be ground is often a poorly controlled factor, yet it strongly influences grinding efficiency. This can be due to lubrication forces and capillary cohesion, which leads to the formation of aggregates that are more difficult to grind. This paper presents an original approach to link the particle aggregation capacity with the grinding rate. This aggregation, which limits the energy available for effective grinding, was estimated using the Carr index. A modified Rittinger law that relates the specific surface area created to the energy transmitted by the grinding media, incorporating the influence of water content is proposed. This model provides new guidelines for achieving more efficient comminution.

#### 1. Introduction

Commonly used across many industrial sectors, grinding is a highly energy-intensive operation [1, 2]. In the mining industry, for instance, electricity consumption related to grinding has recently been estimated to account for approximately 1% of global energy use [3]. The development of particle size reduction technologies (comminution), which dates back to antiquity, remains an incremental and ongoing process. From an operational standpoint, this development primarily aims to achieve two key objectives: to reach a target particle size distribution [4] and to maximize energy efficiency [5]. These objectives are difficult to achieve without accounting for the wide diversity of feed materials, which over time has led to the emergence of a broad range of milling technologies. Indeed, the fundamental mechanisms governing comminution processes can only be fully understood by integrating the complex relationships between process geometry, operating conditions, and the intrinsic properties of the material being ground.

Among these technologies, grinding media mills, such as ball mills, stirred mills, and vibratory mills, are widely used across various industrial sectors, including the food, pharmaceutical, recycling, and mining industries. They offer high operational flexibility and can process a wide range of raw materials, enabling tunable particle size reduction by

ORCID(s): 0009-0009-4830-543X (M. Thouret); 0000-0003-2121-7607 (C. Mayer-Laigle); 0000-0002-8897-5499 (V. Richefeu); 0000-0002-8903-3815 (K. Lampoh); 0000-0002-4107-0502 (J. Delenne)

adjusting grinding time [6, 7]. The evolution of particle populations in grinding media mills results from the complex dynamics of force transmission within the process, propagating from the system's boundary conditions through the grinding media to the particles. At the particle scale, size reduction occurs through mechanical stresses generated by interactions such as impacts, contacts, and friction between grinding bodies, particles, and mill walls. Mechanically, fragmentation occurs when the energy transmitted to a particle exceeds its fracture toughness. The heterogeneous transmission of stress within the mill induces various comminution mechanisms, which can coexist in varying proportions, such as abrasion, cleavage, and shattering [8]. Nevertheless, despite their popularity and ease of use, making them essential tools in industry, grinding media mills suffer from low grinding efficiency [9], with energy losses (i.e., energy not used for comminution) accounting for up to 99 % of the total energy supplied to the mill Lowrison [10].

From a fundamental perspective, research has focused on describing the evolution of particle size distributions during grinding using population balance models [11]. In this context, recent discrete element method (DEM) simulations have demonstrated the feasibility of establishing population balances for simple breakable particles [12]. Such studies are particularly valuable for establishing a direct link between the micromechanics of particle breakage and the macroscopic process of comminution. While providing detailed insight into particle size evolution, population balance approaches often rely on the identification of numerous parameters, which can be difficult to determine experimentally. An alternative, more phenomenological approach involves the use of comminution models, which describe the evolution of particle size (e.g., D50) or specific surface area as a function of input energy. Among the most widely used are the Rittinger, Bond, and Kick laws, which have shown broad applicability across a range of materials and processes [13].

<sup>&</sup>lt;sup>⋆</sup>This document is the results of the research project funded by the U.S. Center for Bioenergy Innovation and the French government FEDER TENABIC project

<sup>\*</sup>Corresponding author

<sup>\*\*</sup>Principal corresponding author

mathis.thouret@inrae.fr (M. Thouret); claire.mayer@inrae.fr (C. Mayer.Jaigle)

In the grinding of natural materials (e.g., ores, plant biomass), poor repeatability is often attributed to the intrinsic variability of the raw materials themselves. This variability is generally seen as an obstacle to the development of generic models. However, it is rarely attributed to external environmental factors such as the presence of water, despite water being more easily quantifiable. Yet water has a strong influence on the rheological behavior of powders, especially when present in small amounts where it forms capillary bridges between particles [14]. Moreover, the presence of water in raw materials is very common, particularly due to the high cost of drying operations. Although dry grinding [15, 16] and fully wet grinding [1] are well documented in the literature, to the best of our knowledge, intermediate water contents have been poorly studied. Furthermore, there is growing interest across various industrial sectors in grinding under unsaturated conditions, for example, in bioenergy production for co-treatment processes [17] or in the cement industry for clay grinding [18]. The state of water in a granular medium strongly depends on the particle size distribution and surface properties, which affect wetting angles and water sorption. In porous media such as plant biomass, water may also be present inside the particles in various forms, from free to structurally bound water. In this triphasic system, several water retention regimes are commonly defined qualitatively: hygroscopic (adsorption of water molecules), pendular (capillary bridges), funicular (formation of water clusters), and capillary (near saturation) [19, 20, 21]. Experimentally, it has been shown across different scientific disciplines, such as chemistry, civil engineering, and mechanics, that internal cohesion exhibits a non-linear relationship with water content [22]. However, understanding the micromechanical origins of the rheology of granular materials across the full range of water contents remains a very active research area in physics [23].

In this paper, the relationship between water content and particle size reduction is examined from a phenomenological perspective. Although the methodology developed here is applicable to a wide range of raw materials, quartz sand was selected as a model material to minimize absorption effects and chemical surface interactions, which can be significant in organic materials. This choice allows to isolate the effects of capillary bonding between water and particles while avoiding confounding factors such as swelling, absorption, water release during grinding, or increased cohesion due to hydrogen bonding between water molecules and polar groups on the feedstock surface. Through vibratory densification tests, the intensity of capillary forces, responsible for generating a negative pressure that holds particles together, is quantified under dynamic conditions and across the full range of water contents. This capillary effect, which limits the transmission of forces and consequently reduces the efficiency of comminution, is non-linear with respect to the water content and reaches a minimum at the point of maximum densification. Using the analytical expression of the mechanical energy transmitted to the powder by the grinding medium proposed by Blanc et al. [24], a linear relationship is observed between the comminution rate and this energy for each water content. Finally, analysis of the relationship between the comminution rate and the densification index makes it possible to propose a general model that extends Rittinger's comminution law over the entire range of water contents, from dry to saturated conditions.

#### 2. Materials and Methods

To characterize the cohesive state of the wet granular material, a three-step methodology is employed: (1) pycnometer tests to determine the water content range of a densely packed sand sample, (2) vibratory densification tests, and (3) grinding experiments across a wide range of water contents.

#### 2.1. Raw material

The sand used for this study is a pre-calibrated quartz sand, sieved between 400  $\mu$ m and 800  $\mu$ m, from Hofer Chemie GmbH®, DE. The median particle size (d50) of the initial feedstock was measured by laser diffraction using a Beckman and Coulter® LS 13320 XR, USA wet way (see section 2.5) with a value  $d50 = 700 \,\mu$ m.

The packing properties of the raw material are also characterized using a vibratory densimeter (Autotap, Quantachrome<sup>®</sup>, USA). The dry tapped density  $\rho$  was determined as the maximum density achieved after applying a sufficient number of taps to reach a steady state in the sample's volume. This characteristic value was reached after approximately 2000 taps. All measurements have been done in triplicate for sample mass of 100g and found an average value of  $\rho \approx 1612 \, \text{kg/m}^3$ .

The intrinsic density  $\rho^*$  was determined, from three measurements, with a nitrogen pycnometer AccuPyc II (Micromeritics<sup>®</sup>, USA) leading to  $\rho^* \approx 2650 \, \text{kg/m}^3$ . This value is typical of quartz material.

# 2.2. Sample preparation at different water content

To cover the full range of possible water contents, It is necessary to define a scale of water masses to be added to a fixed mass of grains. This first requires calculating the maximum quantity of water that can be added without leaving excess water on the surface of the sample.

Following the classical framework of soil mechanics [25], the maximum saturation state is calculated from the dry dense packing configuration of the raw material. In this specific case, the sample is only composed of two phases: air and particles. The total volume of the sample (V) is defined as  $V = V_s + V_v$ , where  $V_s$  is the solid volume and  $V_v$  is the void volume. The total volume can also be expressed as  $V = m_s/\rho$ , and the solid volume as  $V_s = m_s/\rho^*$ , where  $m_s$  is the mass of the solid. The void volume inside the granular packing is thus

$$V_v = \frac{m_s}{\rho} - \frac{m_s}{\rho^*} = \frac{m_s(\rho^* - \rho)}{\rho \rho^*}.$$
 (1)

In the following, the assumption that water is homogeneously distributed in the pore space is made. The mass

of water to add to the sample in order to reach a targeted complete saturation is  $V_w = V_v$ .

A value of water content at saturation  $W_{\rm max}=0.26$  (i.e., 26%) was found for a sample in a dense state. This value will be used in the following to calculate a dimensionless water content:

$$W_a = \frac{W}{W_{\text{max}}} \tag{2}$$

which evolves from 0% in the dry case to 100% for a theoretical saturated sample.

## 2.3. Drying kinetics

For a moist granular material, monitoring water evaporation over time reveals different wetting regimes. In this paper, drying kinetics were carried out using an infrared scale [26] (XM60, Precisa<sup>®</sup>, FR). Three heating temperatures were preliminary tested (80°C, 90°C, and 130°C), all revealing the same characteristic transitions. Therefore, the choice was made to perform all subsequent tests under the boiling point of water at 80°C.

A sample was prepared by mixing the 3 g of sand grains with an amount of water to achieve a target apparent water content  $W_a$  of 100%. The sample was then dried in the infrared scale, and the mass was recorded every 30 seconds. The water content was calculated from the mass loss over time. The measurements were performed in triplicate, showing good repeatability.

#### 2.4. Assessment of the Carr index

The cohesion state of a powder depends on the wetting regime of the granular material. Specifically, binary capillary bridges or water clusters that link more than two particles create interactions between water and sand grains. This occurs due to the combined effect of the negative Laplace pressure within the liquid and the surface tension. This phenomenon can lead to significant material cohesion, which varies non-linearly with water content [27, 14, 28].

In soil mechanics, cohesion is typically quantified using quasi-static triaxial or shear tests, which assess material strength as a function of confining pressure. However, these methods are often complex, time-consuming, and not well suited for capturing capillary forces – especially in granular systems with coarse particles. Moreover, in powder technology, the emphasis is generally placed on dynamic behavior and flowability rather than the rheology under high confining pressure or static stress conditions.

For these reasons, some researchers have proposed vibratory densification tests as a rapid method to quantify powder cohesion [29]. One such approach involves determining the Carr index [30], originally developed for characterizing the flowability of dry powders [31, 32, 33]. It is defined as

$$I_C = \frac{V_i - V_f}{V_i} \tag{3}$$

where  $V_i$  and  $V_f$  are respectively the initial and final volume of the sample. The effect of water content  $W_a$  is considered and thus the Carr index  $I_C$  depends on it:  $I_C(W_a)$ .

A normalized version of the Carr Index is considered, using the dry  $I_C^{\rm dry}=I_C(0\%)$  and maximum  $I_C^{\rm max}$  cases as references:

$$I = \frac{I_C(W_a) - I_C^{\text{dry}}}{I_C^{\text{max}} - I_C^{\text{dry}}} \tag{4}$$

In this paper, Carr index was determined for all water content (in triplicate), by monitoring the volume change of the powder under vibration. A Brüel and Kjaer<sup>®</sup> (DK) vibratory pot is used. It is driven by a sound signal generated from a laptop and amplified to operate the system (Figure 1). This setup provides full control over the vibration frequency, amplitude, and shaking duration. In practice, preliminary tests were performed to identify the optimal parameters for achieving a steady-state packing condition across all water contents: frequency  $f = 20 \,\mathrm{Hz}$ , amplitude  $A = 1 \,\mathrm{mm}$ , and shaking time  $t = 4 \,\mathrm{min}$ .

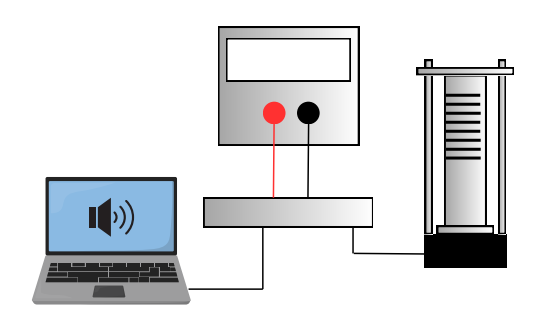


**Figure 1:** Experimental setup for vibratory densification with its signal generator, amplification source and vibration actuator.

# 2.5. Grinding process and particle size measurement

The grinding process was conducted in a MM400 vibratory ball mill with two milling chambers (Retsch<sup>®</sup>, DE), illustrated in Figure 2. The grinding frequency was fixed at 25 Hz. This will allow to compare our results to those obtained by Blanc et al (2020) [24] who performed grinding tests with the same setup (one 20mm stainless steel ball) in dry conditions. Water was added to 13.7 g of quartz sand to reach the appropriate  $W_a$ . Water and sand were mixed and then introduced in the grinding chamber. For each water content and grinding times (0.5 min, 1 min, 2 min, 3 min and 5 min), a small amount of ground powder was sampled to measure the particle size distribution. The grinding times was chosen to be sufficiently low to follow the Rittinger comminution law which corresponds to a linear evolution (fastrate grinding) of the created specific surface as a function time.

The efficiency of the milling process was evaluated by monitoring the evolution of particle size over time using a laser diffraction analyzer (LS 13320 XR, Beckman and Coulter®), based on Mie theory [34, 35].

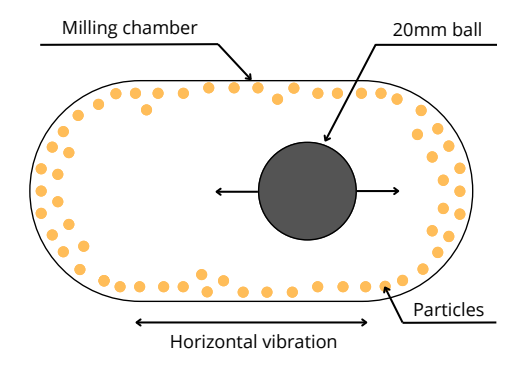


Figure 2: Scheme of vibratory ball mill chamber with the grinding ball and sand particles.

The particle size of sand sampled from each grinding chamber was measured separately, and the resulting particle size distributions were averaged for each experimental condition. To characterize the grinding, two key indicators were used: the median diameter  $D_{50}$  and the specific surface area  $S_s$ , calculated as:

$$S_s = \frac{1}{\rho^*} \sum_i \frac{3\alpha_i}{R_i} \tag{5}$$

where  $\rho^*$  is the intrinsic density of the powder,  $\alpha_i$  is the volumetric fraction of particle size class i, and  $R_i$  is the median radius of class i.

# 3. Experimental results

This section presents the experimental results on the evaluation of densification as a function of water content, and its impact on the efficiency of particle size reduction.

# 3.1. Determination of water regimes

Figure 3 (Top) shows the drying kinetics obtained using an infrared scale, following the protocol described in section 2.3. In Figure 3 (Bottom), the drying rate  $D_r = -\mathrm{d}W_a/\mathrm{d}t$  is plotted as a function of the relative water content  $W_a$ . It highlights three distinct zones that qualitatively correspond to drying regimes.

Zone I, which corresponds to  $W_a$  starting from 100% down to 50%, exhibits a high drying rate that stabilizes rapidly at approximately  $Dr \approx 7\%/\text{min}$ . This phase can be characterized as the **free water regime**, where water is weakly attached to the particles and exposes a large exchange interface on the surface of the wet sand sample. Nevertheless, during evaporation, water within the granular bed undergoes reorganization, gradually resulting in the formation of capillary structures.

Zone II, which manifests as a plateau between 10% and 50%  $W_a$ , is assumed to correspond to the **capillary regime**. In this regime, water aggregates into interparticle clusters, and the water-particle interactions are sufficiently strong to significantly slow down the evaporation rate.

Zone III, observed for relative water content below 10 %, demonstrates a further decrease in drying velocity, though

less pronounced than in Zone I. This regime is indicative of the **pendular and hygroscopic regimes** which correspond to low water contents, ranging from the situation where isolated capillary bridges form at particle contacts to that where water is only adsorbed on surface asperities. The significant interactions between water and particles in this regime increase the difficulty of removing the remaining moisture.

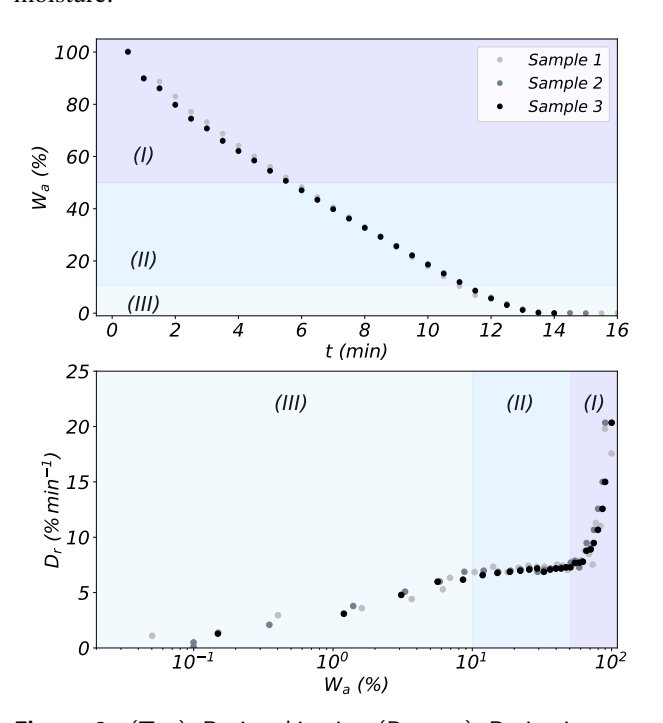


Figure 3: (Top) Drying kinetics (Bottom) Derivative rate evolution

#### 3.2. Vibratory densification

In soil mechanics, soil densification is studied to understand the role of water in the compaction capability of surface soil layers. The so-called Proctor test [36, 37, 38] describes the dry density as a function of water content under a standardized compaction energy. This experiment provides the Optimum Proctor, defined as the water content at which the highest dry density is achieved for a given compaction energy. Following this approach, a slightly different methodology was proposed, based on the Carr index measurement, to identify the optimum densification of granular beds across a range of water contents, from dry to fully saturated conditions.

Figure 4 shows the evolution of I as a function of  $W_a$  for the raw material. A second-order polynomial fit was proposed as follows:

$$I = W_a(a \times W_a + b) \tag{6}$$

where  $a=-3.5.10^{-4}$ ,  $b=3.8.10^{-2}$  ( $R^2=0.99$ ). For low water contents ( $W_a=0\%$  to 40%), an increase in I is observed. This can be attributed to the overgrowth of the powder bed, as experimentally observed, resulting in a greater bulk volume before compaction. This is followed by

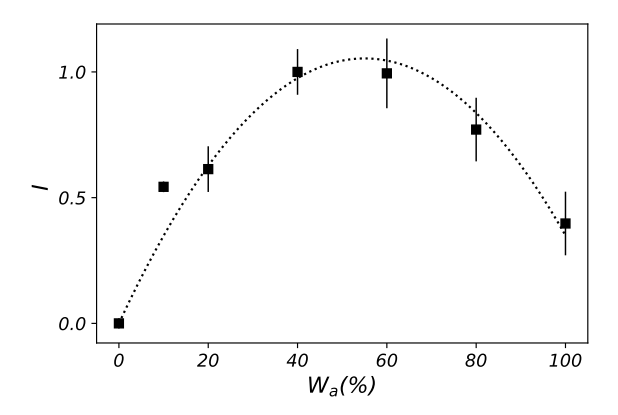


**Figure 4:** I as a function of relative water content  $W_a$ . The dotted curve is parabolic fit used as a guide to the eyes.

a decrease in I. At  $W_a=40\,\%$ , aggregate formation occurs due to strong capillary interactions and a sufficient amount of water to generate tough cohesive aggregates [39]. These aggregates behave similarly to larger particles, producing a more aerated granular structure during the densification test, which results in the highest I.

Beyond  $W_a=40\%$  (corresponding to W=10.4%), a reduction in the number of aggregates and the onset of fluidization phenomena within the sample lead to a decline in I. Interestingly, very similar values can been found in the literature for the Proctor optimum for sand. For example, [40] and [41] found 10.3% and 11.1%, respectively for two similar sands in terms of particle size distribution.

## 3.3. Grinding efficiency

The presence of water significantly impacts particle size reduction during milling. Figure 5 (Top) shows the evolution of the cumulative particle size distribution for different water contents  $W_a$  after 1 minute of grinding, along with the milling kinetics for dry sand over grinding times ranging from 30 seconds to 5 minutes (Bottom). As shown in Figure 5 (Top), increasing the water content from  $W_a = 0\%$  to  $W_a = 40\%$  shifts the grading curves toward coarser particles, indicating reduced comminution efficiency. For  $W_a$  values above 40%, this trend reverses, and the curves tend to resemble those of the dry case.

To better illustrate this behavior, Figure 6 presents the evolution of the median particle diameter,  $D_{50}$ , as a function of water content for different grinding times. From  $W_a=0\,\%$  to  $W_a=40\,\%$ ,  $D_{50}$  clearly increases, reaching a peak around 40 % before decreasing as  $W_a$  approaches 100 %.

It is also noteworthy that the difference in milling efficiency between the dry (or saturated) and the least efficient (for  $W_a=40\,\%$ ) conditions is reduced by a factor of 8 as grinding time increases. This indicates that while water in the unsaturated state initially hinders milling efficiency (requiring four times longer to achieve the same  $D_{50}$  as in the dry case at  $W_a=40\,\%$ ), over time, the  $D_{50}$  values for all water contents tend to converge.

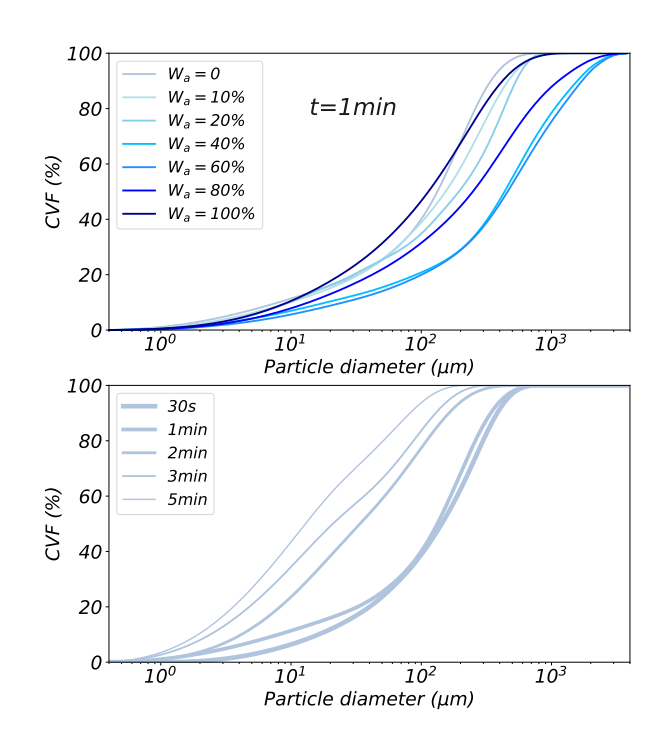


**Figure 5:** Particle size distributions (PSD). (Top) Evolution of cumulated volume fraction (CVF) for  $W_a$  at 1 min grinding time. (Bottom) Grinding kinetic: time evolution of the PSD for dry sand.

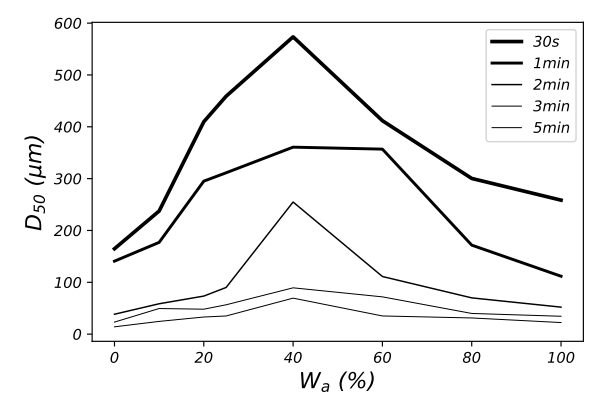


**Figure 6:** Evolution of  $D_{50}$  as a function of  $W_a$  for different grinding times.

## 4. Comminution model

Various comminution laws have been proposed to describe particle size reduction in granular media [13]. Among the most well-known are the Bond, Kick, and Rittinger models. These laws provide effective modeling of specific surface area generation as a function of grinding energy in the case of dry granular materials. In this paper, an adaptation of the Rittinger model that accounts for the presence of water

within the feedstock is proposed. The study focus on short grinding times, during which the evolution of the specific surface area S with respect to energy remains approximately linear, allowing to define a constant grinding rate.

# 4.1. Grinding energy for dry sand

By assuming that the ball-chamber impact occurs without dissipation at maximal velocity for both the ball and the chamber. This corresponds to a reference impact energy of  $8m_b(A\pi f)^2$ , where  $m_b$  is the mass of the ball, A is the amplitude of oscillation of the grinding chamber, and f is the oscillation frequency of the chamber. The specific grinding energy  $E_m$  corresponds thus to this specific impact energy divided by the dry mass of the feedstock M, and multiplied by the number of impacts ft during the grinding time t. Hence, as proposed by Blanc et al. [24], the specific grinding energy induced by the ball in the vibratory ball mill (MM400) reads:

$$E_m(t) = \frac{16 \, m_b \big( A \pi \big)^2 f^3}{M} \, t \tag{7}$$

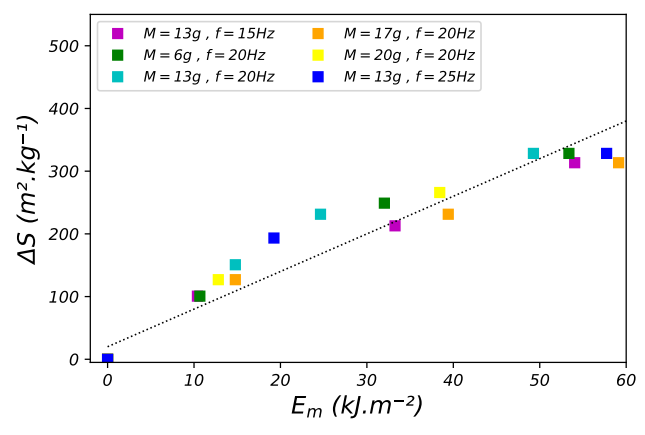


Figure 7: Evolution of the gain in specific surface  $\Delta S = S - S_0$  with respect to the specific grinding energy for dry sand; data from Blanc et al. [24]. The dotted line is a linear regression where the slope is the Rittinger constant  $\tau_0 = \Delta S / E_m$ .

Figure 7 presents data from Blanc et al. [24], illustrating the linear relationship between the gain in specific surface per unit mass of feedstock, denoted as  $\Delta S$ , and the specific grinding energy,  $E_m$ . This relationship has been examined across various feedstock quantities and frequencies. The data aligns with the Rittinger model, which is particularly applicable during the initial phase of fine comminution, and can be expressed by the relation:

$$\Delta S = \tau_0 E_m \tag{8}$$

where the Rittinger constant  $\tau_0$  is approximately  $6 \, \text{m}^2 \text{kJ}^{-1}$ .

# 4.2. Wet grinding model

This section is now focused on assessing the impact of incorporating water into the granular material prior to grinding. For comparison, It was decided to use process settings similar to those in one of the test series mentioned by Blanc et al. [24]:  $m_b = 32.7$  g,  $A = 7.20 \pm 0.05$  mm, and f = 25 Hz.

Figure 8 illustrates the evolution of the specific surface, similar to Figure 7, but with varying values of  $W_a$ . Only the initial linear portion is displayed.

A distinct impact of water content is evident from the variations in slope for different water levels, indicating that the Rittinger constant is influenced by  $W_a$ .

The presence of water introduces several forces at the contact level, including capillary and viscosity. These forces can hinder energy transfer and, as a result, decrease the effectiveness of the milling process.

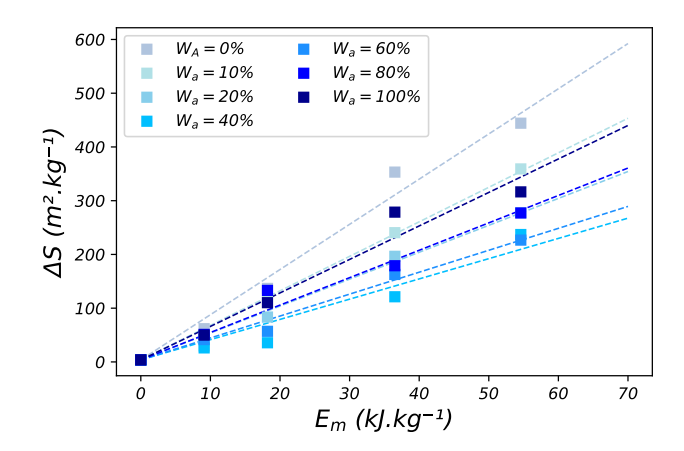
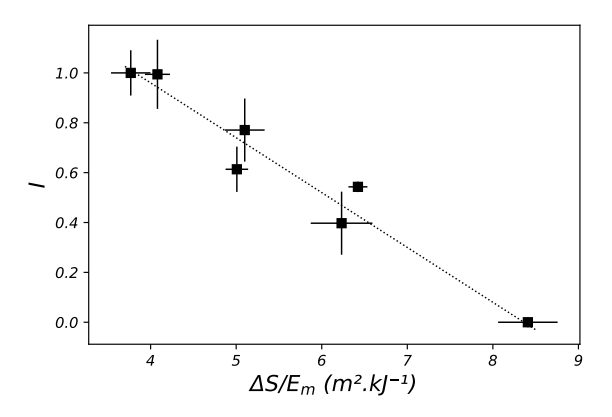


Figure 8: Evolution of  $\Delta S$  according to  $E_m$  for different  $W_a$ .

Therefore, the relationship between grinding efficiency and the alteration of the sand state caused by the presence of water needs to be explored. Since the normalized Carr index I can be measured through simple experiments, it appears to be a reliable indicator of the sand state. To verify this, I against the grinding rate  $\Delta S/E_m$  is plotted in Figure 9. A fairly clear linear decrease in I is observed, suggesting that it is related to the initial grinding efficiency.



**Figure 9:** Correlation between the relative Carr index I for wet sand and the grinding efficiency expressed as the Rittinger constant  $\Delta S/E_m$ , as it is defined for dry sand.

Starting from this observation, this paper proposed a modified Rittinger model that takes into account the presence of water. First, the expression of the specific grinding energy, initially proposed by [24] for the dry case needs to be adjusted, to apply to the wet case.

Adding water to the feedstock means the total mass M is the sum of the mass of sand and the mass of water. Given the definition of water content  $W = m_{\text{water}}/m_{\text{sand}}$  and the relative water content  $W_a = W/W_{\text{max}}$ , the mass of the feedstock in the wet case is expressed as:

$$M = m_{\text{sand}}(1 + W_a W_{\text{max}}) \tag{9}$$

In wet conditions, the specific grinding energy is expressed as:

$$\hat{E}_m(W_a, t) = \frac{16 m_b (A\pi)^2 f^3}{m_{\text{sand}} (1 + W_a W_{\text{max}})} t$$
 (10)

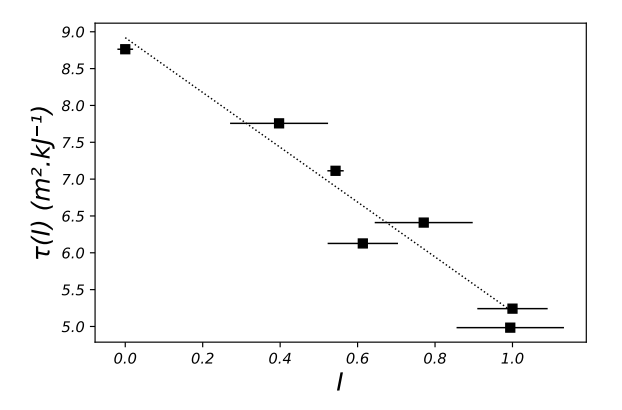


**Figure 10**: Evolution of  $\tau(I)$  as function of I

The grinding efficiency can thus be calculated as a function of I:

$$\tau(I) = \frac{\Delta S}{\hat{E}_{m}} \tag{11}$$

Figure 10 illustrates the evolution of  $\tau$  with respect to I.

Given the measurement tolerances, an affine relationship effectively captures the relationship between  $\tau$  and I, which can be fitted as follows:

$$\tau(I) = \chi I + \tau^0 \tag{12}$$

with  $\chi = -3.6 \,\mathrm{m}^2 \mathrm{kJ}^{-1}$  and  $\tau^0 = 9 \,\mathrm{m}^2 \mathrm{kJ}^{-1}$ .

By combining Equations (10) and (12) in the modified Rittinger model  $\Delta S = \tau(I)\hat{E}_m$ , the predicted gain in specific surface  $\Delta S_p$  under wet conditions can be expressed using the following adapted relation:

$$\Delta S_{\rm p} = (\chi I + \tau^0) \, \hat{E}_m \tag{13}$$

Figure 11 shows a comparison between the measured and predicted gains in specific surface across different water contents. The close clustering of data points along the line  $\Delta S = \Delta S_p$  highlights the strong agreement between experiment and model prediction given in Equation (13).

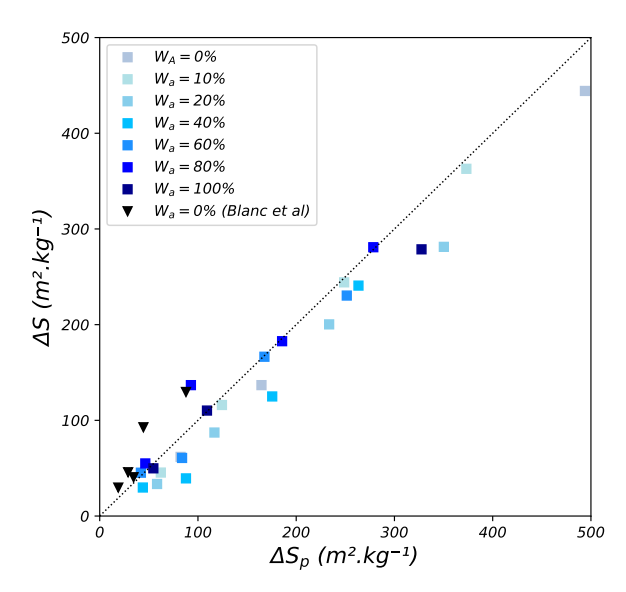


Figure 11: Comparison of predicted  $(\Delta S_p)$  versus measured  $(\Delta S)$  gains in specific surface when grinding wet sand.

# 5. Conclusion and perspectives

The primary conclusion of this study is highly relevant to grinding processes involving wet feedstock. It is observed that grinding efficiency decreases almost linearly as the Carr Index increases. However, the Carr Index reaches its maximum at a relative water content of approximately 40%. It decreases both when the water content is reduced (drying) and when it is increased (by adding water). Therefore, to improve the grinding performance of an initially wet feedstock, adding water, rather than drying the material, may offer a simpler and more energy-efficient solution.

Several studies in the literature have examined the effect of water content on the strength of granular media through both experimental and numerical investigations [27, 42, 28]. Indeed, the presence of water clustering within a granular material generates capillary forces that "glue" particles together. These capillary forces induce cohesion at the macroscale, which varies as a function of water content. Interestingly, it has been shown in the literature that this cohesion reaches a maximum value for an intermediate water content ranging between 5% and 15%. In this article, the affinity of water molecules for binding to the porous surface of the sand bed was qualitatively demonstrated through the study of drying kinetics (Figure 3). Starting from a fully saturated sample, it was shown that the evaporation rate drops sharply before reaching a plateau at approximately  $W_a \approx 40\%$ . This value marks the transition between two regimes: the first, where water is free and present in excess, and the second, where liquid and gas phases coexist in significant proportions. In this domain, clusters of water tend to promote particle aggregation. For  $W_a < 5\%$ , capillary and hygroscopic interactions dominate; however, due to the very low water content, the resulting aggregates are weak and short-lived. The choice of an indicator is required to characterize grinding efficiency in the presence of water. However, this investigation was motivated by two key considerations:

- Drying kinetics alone are insufficient to fully capture the cohesive forces driving aggregation. The spatial distribution of the liquid phase, particularly the formation of clusters, plays a critical role in cohesion, as demonstrated by [28, 43, 44].
- The cohesion measured using a rheometer (FT4 or Schulze [e.g., 45, 46]) or a shear device (Casagrande or Jenike cell [e.g., 47, 48]) does not reflect dynamic behavior, but rather represents a steady state or quasistatic shear resistance measured at zero confinement pressure.

Consequently, in this work, the Carr index was selected as an indicator of grinding efficiency, and the relationship between the Carr index and the comminution rate over the entire range of water content was examined.

Indeed, the Carr index represents the densification capability of a granular sample subjected to vertical vibration. At approximately  $W_a \approx 40\%$ , the loosest samples were observed, composed of large plastic aggregates due to efficient capillary cohesion. In this case, relative compaction under vibration is highest, leading to the maximum value of the Carr index.

Interestingly, It was shown that the water content corresponding to this maximum Carr index is associated with less efficient comminution. Indeed, the continuous formation and breakage of aggregates during the grinding process tends to limit the overall energy available for breaking individual particles (Figure 6).

Consequently, a higher  $D_{50}$  is observed for all milling times at a water content  $W_a$  of 40%. Interestingly, beyond this point of maximum densification, the comminution efficiency steadily improves, and the particle size reduction eventually becomes comparable to that of the dry case at  $W_a = 100\%$ 

A model has been proposed to capture this trend, building on previous work that describes the dry case (Blanc et al.). This model relates the creation of specific surface area to grinding energy through a linear correlation, incorporating the densification state via two simple input parameters: the amount of added water and the Carr index. The agreement between experimental and predicted data is very good for relatively short milling times, where the grinding kinetics (specific surface area as a function of cumulative grinding energy) remain linear.

At longer grinding times, the grinding kinetics tend to level off due to the increasing influence of cohesive forces. This comminution regime, which has been little studied due to its low efficiency, remains of interest for applications requiring ultra-fine milling. It will be examined in detail in future work. Greater accuracy can be achieved by adjusting the Carr index throughout the grinding process.

Additionally, other forces, such as lubrication forces, may influence particle size reduction at longer grinding

times. The relative impact of lubrication compared to capillary and contact forces could be assessed using Discrete Element Method (DEM) simulations.

Finally, the methodology proposed in this paper will be applied to a broad range of feedstocks, including organic materials for which sorption phenomena play a significant role. One target material is plant biomass, composed of cell walls that are highly sensitive to moisture and are typically processed using semi-wet grinding methods, particularly in biofuel applications.

# **Declaration of Competing Interest**

The authors declare that they have no known competing financial interests or personal relationships that could have appeared to influence the work reported in this paper.

# Acknowledgements

The authors thank the technological platform Planet for the technical support during the experimental study: https://doi.org/10.15454/1.5572338990609338E12 The authors thanks US Center for Bioenergy Innovation and french Feder Tenabic project for their financial support.

# **CRediT** authorship contribution statement

Mathis Thouret: Conceptualization, Methodology, Experiments, Writing - Original Draft. Claire Mayer-Laigle: Conceptualization, Methodology, Writing - Original Draft. Vincent Richefeu: Conceptualization, Methodology, Writing - Original Draft. Komlanvi Lampoh: Conceptualization, Methodology, Writing - Original Draft. Jean-Yves Delenne: Conceptualization, Methodology, Writing - Original Draft.

## References

- [1] T Yu, J Sun, J Li, A Wang, M Nie, X Gong, L Wang, L Liu, F Wang, and L Tong. Effects of milling methods on rice flour properties and rice product quality: A review. *Rice Science*, 31(1):33–46, 2024.
- [2] A Paul, L Lopez-Vidal, and AJ Paredes. Progress in the production of nanocrystals through miniaturised milling methods. RPS Pharmacy and Pharmacology Reports, pages rqaf008, 2025.
- [3] Weir. Mining energy consumption report. Technical report, Weir Group, 2021.
- [4] Rolands Cepuritis, Edward J. Garboczi, Chiara F. Ferraris, Stefan Jacobsen, and Bjørn E. Sørensen. Measurement of particle size distribution and specific surface area for crushed concrete aggregate fines. Advanced Powder Technology, 28(3):706–720, 2017.
- [5] T Zhang, Z Liu, X Sun, J Xu, L Dong, and G Zhu. Investigation on specific milling energy and energy efficiency in high-speed milling based on energy flow theory. *Energy*, 192:116596, 2020.
- [6] A Rizzo and GI Peterson. Progress toward sustainable polymer technologies with ball-mill grinding. *Progress in Polymer Science*, 159:101900, 2024.
- [7] C Mayer-Laigle, RK Rajaonarivony, N Blanc, and X Rouau. Comminution of dry lignocellulosic biomass: Part II. Technologies, improvement of milling performances, and security issues. *Bioengineering*, 5(3):50, 2018.
- [8] Maruf Hasan, Sam Palaniandy, Marko Hilden, and Malcolm Powell. Calculating breakage parameters of a batch vertical stirred mill. *Minerals Engineering*, 111:229–237, 2017.

- [9] Stefano Martelli and Paolo Emilio Di Nunzio. Powder ball milling: An energy balance approach to particle size reduction. *Journal of Materials Research*, 40(2):292–308, 2025.
- [10] GC Lowrison. The size reduction of solid materials. crushing and grinding, 1974.
- [11] Brena Karolyne N. Rocha, Túlio M. Campos, and Luís Marcelo Tavares. Modelling multicomponent breakage and liberation by detachment of an iron ore in batch ball milling. *Minerals Engineering*, 232:109573, 2025.
- [12] Luisa Fernanda Orozco, Duc-Hanh Nguyen, Jean-Yves Delenne, Philippe Sornay, and Farhang Radjai. Discrete-element simulations of comminution in rotating drums: Effects of grinding media. *Powder Technology*, 362:157–167, 2020.
- [13] LG Austin. A commentary on the kick, bond and rittinger laws of grinding. *Powder Technology*, 7(6):315–317, 1973.
- [14] Vincent Richefeu, F Radjaı, and Moulay Said El Youssoufi. Stress transmission in wet granular materials. *The european physical journal E*, 21:359–369, 2006.
- [15] Danna Shan, Shubo Deng, Tianning Zhao, Bin Wang, Yujue Wang, Jun Huang, Gang Yu, Judy Winglee, and Mark R Wiesner. Preparation of ultrafine magnetic biochar and activated carbon for pharmaceutical adsorption and subsequent degradation by ball milling. *Journal of Hazardous Materials*, 305:156–163, 2016.
- [16] Shivangi Naik and Bodhisattwa Chaudhuri. Quantifying dry milling in pharmaceutical processing: a review on experimental and modeling approaches. *Journal of pharmaceutical sciences*, 104(8):2401–2413, 2015.
- [17] Anahita Bharadwaj, Evert K Holwerda, John M Regan, Lee R Lynd, and Tom L Richard. Enhancing anaerobic digestion of lignocellulosic biomass by mechanical cotreatment. *Biotechnology for Biofuels and Bioproducts*, 17(1):76, 2024.
- [18] Xingyang He, Zhengqi Zheng, Mengyang Ma, Ying Su, Jin Yang, Hongbo Tan, Yingbin Wang, and Bohumír Strnadel. New treatment technology: The use of wet-milling concrete slurry waste to substitute cement. *Journal of Cleaner Production*, 242:118347, 2020.
- [19] Luc Scholtès, P-Y Hicher, François Nicot, Bruno Chareyre, and Félix Darve. On the capillary stress tensor in wet granular materials. *International journal for numerical and analytical methods in geome-chanics*, 33(10):1289–1313, 2009.
- [20] Ning Lu, M Asce, and William Likos. Suction stress characteristic curve for unsaturated soil. *Journal of Geotechnical and Geoenvi*ronmental Engineering - J GEOTECH GEOENVIRON ENG, 132, 02 2006. doi: 10.1061/(ASCE)1090-0241(2006)132:2(131).
- [21] E. Rondet, M. Delalonde, T. Ruiz, and J.P. Desfours. Hydro-textural and dimensional approach for characterising wet granular media agglomerated by kneading. *Chemical Engineering Research and Design*, 86(6):560–568, 2008. ISSN 0263-8762. doi: https://doi.org/ 10.1016/j.cherd.2008.02.020. URL https://www.sciencedirect.com/ science/article/pii/S0263876208000476. 11th Congress of the French Chemical Engineering Society.
- [22] Vincent Richefeu, Moulay Said El Youssoufi, and Farhang Radjai. Shear strength properties of wet granular materials. *Physical Review E—Statistical, Nonlinear, and Soft Matter Physics*, 73(5):051304, 2006.
- [23] Sandip Mandal, Maxime Nicolas, and Olivier Pouliquen. Insights into the rheology of cohesive granular media. *Proceedings of the National Academy of Sciences*, 117(15):8366–8373, 2020. doi: 10.1073/pnas.1921778117. URL https://www.pnas.org/doi/abs/10. 1073/pnas.1921778117.
- [24] Nicolas Blanc, Claire Mayer-Laigle, Xavier Frank, Farhang Radjai, and Jean-Yves Delenne. Evolution of grinding energy and particle size during dry ball-milling of silica sand. *Powder Technology*, 376: 661–667, 2020.
- [25] JK Mitchell and K Soga. Fundamentals of soil behavior. 2005.
- [26] Ipsita Das, SK Das, and Satish Bal. Drying kinetics of high moisture paddy undergoing vibration-assisted infrared (ir) drying. *Journal of Food Engineering*, 95(1):166–171, 2009.

- [27] Mario Scheel, Ralf Seemann, Martin Brinkmann, M. Di Michiel, A Sheppard, B Breidenbach, and Stephan Herminghaus. Morphological clues to wet granular pilestability. *Nature materials*, 7:189–93, 04 2008. doi: 10.1038/nmat2117.
- [28] Jean-Yves Delenne, Vincent Richefeu, and Farhang Radjai. Liquid clustering and capillary pressure in granular media. *Journal of Fluid Mechanics*, 762:R5, 2015.
- [29] Horng Yuan Saw, Clive E Davies, Anthony HJ Paterson, and Jim R Jones. Correlation between powder flow properties measured by shear testing and hausner ratio. *Procedia engineering*, 102:218–225, 2015.
- [30] Ralph L Carr. Evaluating flow properties of solids. Chemical engineering, 72:163–168, 1965.
- [31] Muhammad Ali Kaleem, Muhammad Zubair Alam, Mushtaq Khan, Syed Husain Imran Jaffery, and Badar Rashid. An experimental investigation on accuracy of hausner ratio and carr index of powders in additive manufacturing processes. *Metal Powder Report*, 76:S50– S54, 2021.
- [32] James B Knight, Edward E Ehrichs, Vadim Yu Kuperman, Janna K Flint, Heinrich M Jaeger, and Sidney R Nagel. Experimental study of granular convection. *Physical Review E*, 54(5):5726, 1996.
- [33] N Stanley-Wood, M Sarrafi, Z Mavere, and M Schaefer. The relationships between powder flowability, particle re-arrangement, bulk density and jenike failure function. Advanced Powder Technology, 4 (1):33–40, 1993
- [34] Gerben BJ de Boer, Cornelis de Weerd, Dirk Thoenes, and Hendrik WJ Goossens. Laser diffraction spectrometry: Fraunhofer diffraction versus mie scattering. *Particle & Particle Systems Characteriza*tion, 4(1-4):14–19, 1987.
- [35] He Li, Jingwen Li, Jeffrey Bodycomb, and Gregory S Patience. Experimental methods in chemical engineering: particle size distribution by laser diffraction—psd. *The Canadian Journal of Chemical Engineering*, 97(7):1974–1981, 2019.
- [36] Joshua Connelly, Wayne Jensen, and Paul Harmon. Proctor compaction testing. 2008.
- [37] LE Wagner, NM Ambe, and D Ding. Estimating a proctor density curve from intrinsic soil properties. *Transactions of the ASAE*, 37(4): 1121–1125, 1994
- [38] Robert W Day, Gordon P Boutwell, Craig H Benson, and Lisa R Blotz. Estimating optimum water content and maximum dry unit weight for compacted clays. *Journal of Geotechnical and Geoenvironmental Engineering*, 126(2):195–197, 2000.
- [39] E Rondet, M Delalonde, T Ruiz, and JP Desfours. Identification of granular compactness during the kneading of a humidified cohesive powder. *Powder technology*, 191(1-2):7–12, 2009.
- [40] Brad Joseph Arcement, Stephen G Wright, et al. Evaluation of laboratory compaction procedures for specification of densities for compacting fine sands. Technical report, United States. Federal Highway Administration, 2001.
- [41] Maria Jolanta Sulewska and Dariusz Tymosiak. Analysis of compaction parameters of the exemplary non-cohesive soil determined by proctor methods and vibrating table tests. *Annals of Warsaw University of Life Sciences-SGGW. Land Reclamation*, 50(2), 2018.
- [42] Vincent Richefeu, Moulay Said El Youssoufi, Robert Peyroux, and Farhang Radjai. A model of capillary cohesion for numerical simulations of 3d polydisperse granular media. *International Journal for Numerical and Analytical Methods in Geomechanics*, 32(11):1365– 1383, 2008.
- [43] Vincent Richefeu, Farhang Radjai, and Jean-Yves Delenne Lattice Boltzmann modelling of liquid distribution in unsaturated granular media. *Computers and Geotechnics*, 80:353–359, 2016.
- [44] R. Hosseini, K. Kumar, and J.-Y. Delenne Investigating the source of hysteresis in the soil-water characteristic curve using the multiphase lattice boltzmann method. arXiv, 220407174, 2022.
- [45] R. Freeman. Measuring the flow properties of consolidated, conditioned and aerated powders A comparative study using a powder rheometer and a rotational shear cell. *Powder Technology*, 174(1): 25–33, 2007. Special Edition from the PSA2005 Conference.

- [46] D. Schulze. Shear testing of powders for process optimization. Annual Transactions of the Nordic Rheology Society, 21:99–106, 2013.
- [47] V. Richefeu, M. S. El Youssoufi, R. Peyroux, and C. Bohatier. Frictional contact and cohesion laws for Casagrande's shear test on granular materials by 3D DEM-comparison with experiments. *Powders and Grains*, 5:1–4, 2005.
- [48] Haim Kalman and Dmitry Portnikov. Underwater measurements of flowability by angle of repose, Hausner ratio and Jenike shear cell. *Powder Technology*, 429:118883, 2023.